

Supporting Information

Water Droplet Motion Control on Superhydrophobic Surfaces: Exploiting the Wenzel-to-Cassie Transition

Guangming Liu,[†] Lan Fu,[‡] Andrei V. Rode,[§] Vincent S. J. Craig^{†,*}

[†]*Department of Applied Mathematics, Research School of Physics and Engineering, The Australian National University, Canberra, ACT 0200, Australia*

[‡]*Department of Electronic Materials Engineering, Research School of Physics and Engineering, The Australian National University, Canberra, ACT 0200, Australia*

[§]*Laser Physics Centre, Research School of Physics and Engineering, The Australian National University, Canberra, ACT 0200, Australia*

* To whom correspondence should be addressed. E-mail: vince.craig@anu.edu.au.

Experiments Conducted on a Second Substrate

We have also investigated the Wenzel-to-Cassie transition and the subsequent motion of water droplets on a second micropatterned substrate that has different surface features including the pillar height, the pillar top surface area and the distance between the pillars (Figure S1) to show that the phenomena observed in our experiments is a general effect and not dependent on the precise geometry of the surface employed. A square pattern was defined on the GaAs substrate as for the first substrate however the size of $50\ \mu\text{m} \times 50\ \mu\text{m}$, with a targeted depth of $\sim 13\ \mu\text{m}$ was used for the second substrate.

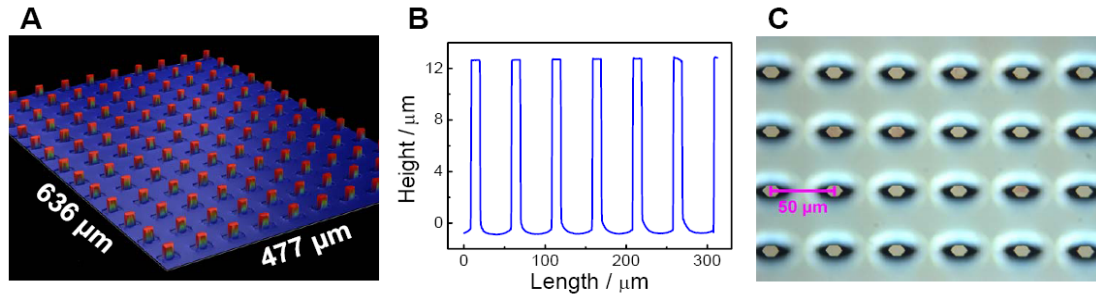


Figure S1. Characterization of the second micropatterned substrate. **(A)** An image obtained by surface profilometry depicting the three-dimensional nature of the substrate. **(B)** A cross-section of the substrate also obtained by surface profilometry. **(C)** A top view of the substrate obtained by optical microscopy. The θ_C is $\sim 145^\circ$ based on calculations using the surface parameters presented here. The Wenzel state is an energetically favored state in comparison with the Cassie state for this surface since the θ_C is larger than the θ_S ($\sim 110^\circ$).

Both the Cassie state and the Wenzel state can coexist on the second micropatterned hydrophobised substrate (see Figure S2). The Cassie state ($\theta_S \sim 161^\circ$) is obtained by depositing a water droplet ($\sim 6 \mu\text{L}$) gently on the surface, whereas the Wenzel state ($\theta_S \sim 119^\circ$) is obtained by releasing a water droplet ($\sim 6 \mu\text{L}$) from a height of $\sim 1 \text{ cm}$ onto the surface (impact velocity $\sim 0.44 \text{ m/s}$). The light cannot be seen between the droplet and the surface in the Cassie state because the space is too narrow between the droplet and the surface, and between the pillars. The contact angle hysteresis for the surface in the Cassie state is $\sim 9^\circ$ ($\theta_A \sim 165^\circ/\theta_R \sim 156^\circ$), whereas the contact angle hysteresis in the Wenzel state is $\sim 63^\circ$ ($\theta_A \sim 135^\circ/\theta_R \sim 72^\circ$).

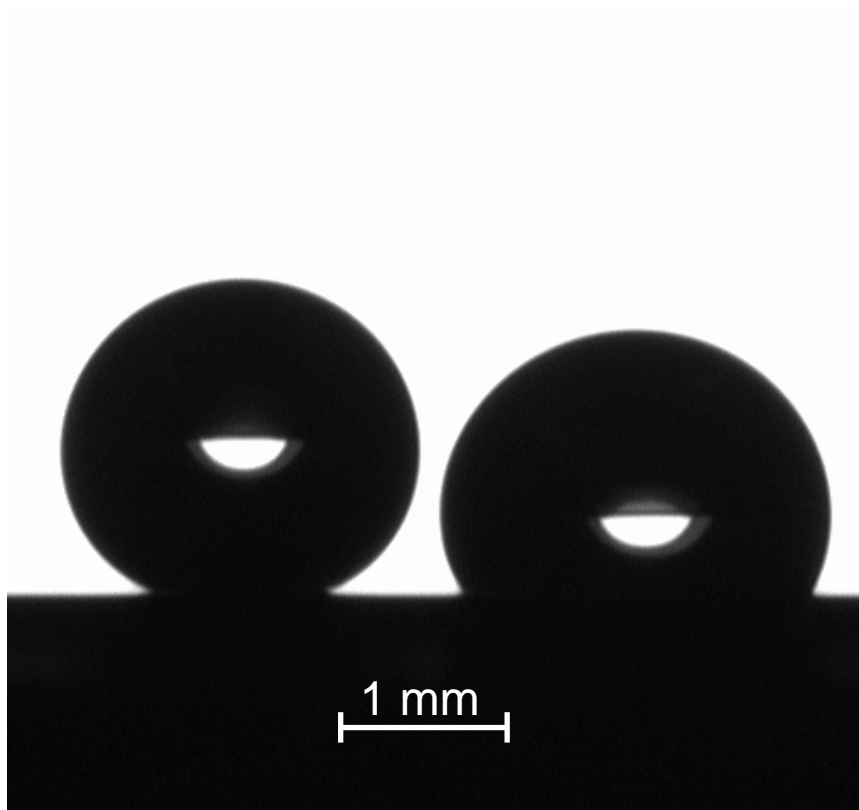


Figure S2. Both the Cassie state (left) and the Wenzel state (right) can coexist on the second micropatterned hydrophobised substrate. Note that the light cannot be seen between the droplet and the surface in the Cassie state because the gap between the droplet and the surface and between the pillars is too small. As with the first substrate the Wenzel to Cassie transition could be effected on the second substrate by heating, and the subsequently selective motion of water droplets on the tilted superhydrophobic surfaces could also be achieved by the local application of heat.

Videos of Motion Control of Droplets on the First Substrate

1. V1: a side view of the Wenzel-to-Cassie transition and the subsequent motion of one water droplet ($\sim 4 \mu\text{L}$) out of two droplets on the tilted substrate. The

transition was induced by local heating using a soldering iron applied to the underside of the substrate.

2. V2: a top view of the Wenzel-to-Cassie transition and the subsequent motion of first one water droplet ($\sim 4 \mu\text{L}$) and then another one on the tilted substrate. The transition was induced by local heating using a soldering iron applied to the underside of the substrate.
3. V3: a top view of the Wenzel-to-Cassie transition and the subsequent motion of one water droplet ($\sim 4 \mu\text{L}$) from a selection of four droplets on the tilted substrate. The transition was induced by local heating using a soldering iron applied to the underside of the substrate.
4. V4: a top view of the Wenzel-to-Cassie transition and the subsequent motion of first one water droplet ($\sim 4 \mu\text{L}$) and then another from three droplets on the tilted substrate. The transition was induced by local heating using a soldering iron applied to the underside of the substrate.
5. V5: a side view of the Wenzel-to-Cassie transition and the subsequent motion of one water droplet ($\sim 4 \mu\text{L}$) on the tilted substrate. The transition was induced by directly heating the droplet using a laser incident upon the underside of the substrate.
6. V6: a side view of the Wenzel-to-Cassie transition and the subsequent motion of one water droplet ($\sim 4 \mu\text{L}$) out of two droplets on the tilted substrate. The transition was induced by directly heating the droplet using a laser incident upon the underside of the substrate.